



## Precision Analysis of Chain Wheel Geometry Reconstruction Based on Contact and Optical Measurement Data



Paweł Turek<sup>\*</sup> , Jakub Jędras 

Faculty of Mechanical Engineering and Aeronautics, Rzeszów University of Technology, 35-959 Rzeszów, Poland

\* Correspondence: Paweł Turek (pturek@prz.edu.pl)

Received: 04-20-2023

Revised: 05-12-2023

Accepted: 05-28-2023

**Citation:** P. Turek and J. Jędras, "Precision analysis of chain wheel geometry reconstruction based on contact and optical measurement data," *J. Eng. Manag. Syst. Eng.*, vol. 2, no. 2, pp. 108–116, 2023. <https://doi.org/10.56578/jemse020202>.



© 2023 by the authors. Licensee Acadlore Publishing Services Limited, Hong Kong. This article can be downloaded for free, and reused and quoted with a citation of the original published version, under the CC BY 4.0 license.

**Abstract:** This study focuses on the detailed reconstruction of chain wheel geometry utilizing measurement data gathered from the MarSurfXC20 contact system and the iNEXIVE VMA 2520 optical system. Supplementary data were also gathered from a digital micrometer and a caliper to provide a comprehensive data set for the analyzed geometry. The geometric model of the chain wheel was then constructed using Siemens NX software. The reconstructed model was subsequently compared with the original design specifications to assess the fidelity of the reconstructed model. Results demonstrate a high degree of correlation between the model generated by reverse engineering and the original design model. Despite the satisfactory correlation, potential inaccuracies were identified, necessitating further research to mitigate these discrepancies and optimize the procedures for parameters beyond the established tolerance. The study affirms the feasibility of utilizing contact and optical measuring systems in the reverse engineering process of chain wheel geometry, although it underscores the need for additional refinement to improve the model's accuracy.

**Keywords:** Coordinate measurement systems; Chain wheel geometry; Reverse engineering; Model accuracy; Computer-Aided Design (CAD) modelling

### 1 Introduction

Computer-Aided Design (CAD), a standard in current industrial processes, enables the swift creation of digital models [1–3]. A problem arises when there is a dearth of technological, construction, or material documentation for a particular product. The advent of coordinate measuring systems, data processing software, and modern manufacturing techniques has, however, paved the way for an effective solution to this problem - Reverse Engineering (RE) [4, 5].

RE is an innovative process that facilitates the creation of 2D documentation from a physical object. It encompasses the measurement and reconstruction of the object's geometry to extrapolate construction-related information. The transformation of a physical object into 2D documentation and a 3D model is contingent on the measuring devices and software used. The resultant technical documentation can serve as a foundation for manufacturing, archiving, or quality control processes. The applications of RE are wide-ranging, encompassing aviation [6], automotive [7], and architectural fields [8]. Its utilities are further witnessed in the medical sector, where it is employed in the reconstruction of anatomical structures' geometry [9–11], design of implants [12–14], surgical templates [15, 16], and scaffolds [17].

The precision of model geometry reconstruction is influenced by each stage of the RE process [4, 5]. Data acquisition, a pivotal stage, necessitates the appropriate selection of the system, parameters, and measurement strategy. Both contact [18, 19] and optical measurements [20, 21] are employed currently to digitize the required geometric dimensions. The resulting data can either represent a 2D image [9, 10], a 2D [18, 19], or a 3D point cloud [21]. Subsequent data processing typically commences with a digital filtering process that eliminates measurement noise [22], leading to a comprehensive representation of the model geometry. Generally, the reconstructed geometry is triangulated [23, 24], with potential for further modeling that includes covering the polygonal mesh with elementary surface patches [25]. The resulting model can be utilized to execute a machining program on numerically controlled machine tools. Accurately estimating errors occurring at the stage of geometry reconstruction presents a

challenge. This study delineates a comparison of the parameters of the chain wheel as obtained in the design process with those garnered in the RE process.

## 2 Methodology

The process of geometry reconstruction was applied to a duplex chain wheel from a Ford Transit 2000 - 2004. Geometric dimensions were collected utilizing a contact coordinate system, the MarSurf XC 20, supplemented by an optical iNEXIVE VMA 2520 microscope. Manual instruments, such as a caliper and micrometer, were also employed to gather additional measurements.

The MarSurf XC 20 in subgraph (a) of Figure 1, with its advanced contour measurement technology, facilitated the efficient measurement of the profile. Composed of a measuring table and a drive unit inclusive of an arm and a measuring head, the MarSurf XC 20 was adapted to the shape and size of the measured object. The measuring head, controlled by PC-installed software, moved in one plane along the measurement section, defined by the machine operator. The measurement of the chain wheel's geometric features, specifically the external in subgraph (b) of Figure 1, internal in subgraph (c) of Figure 1, surface contour, and teeth contour in subgraph (d) of Figure 1 was conducted at the lowest available speed of 0.2 mm/s with the highest resolution of 0.001 mm.

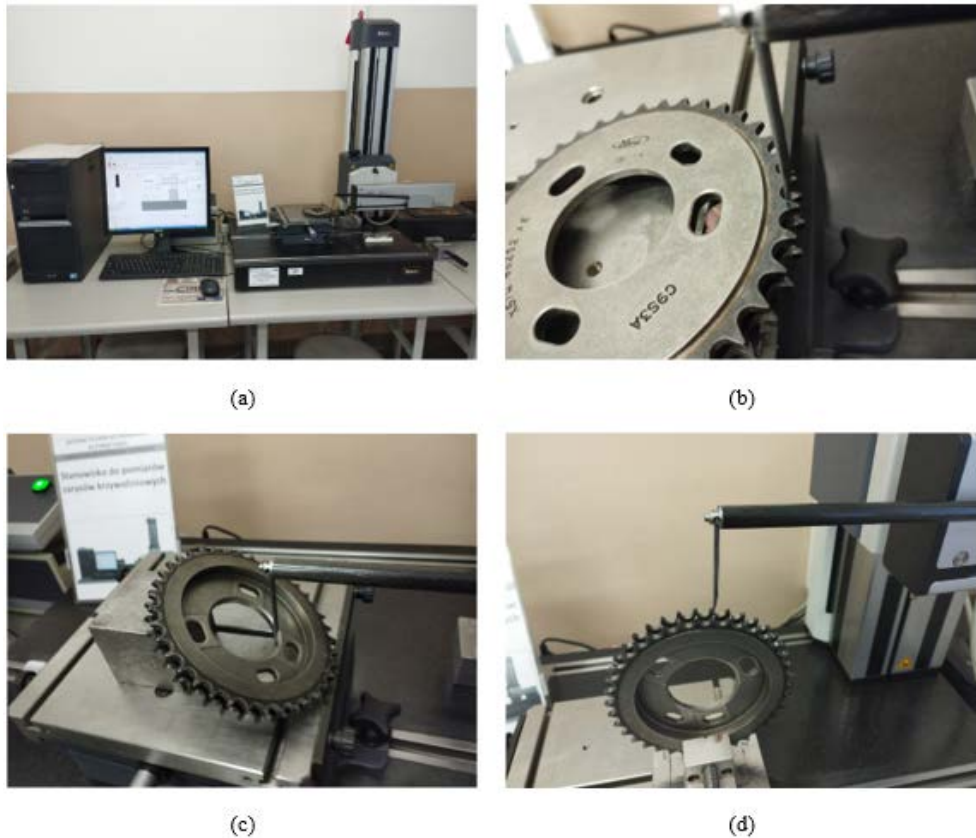
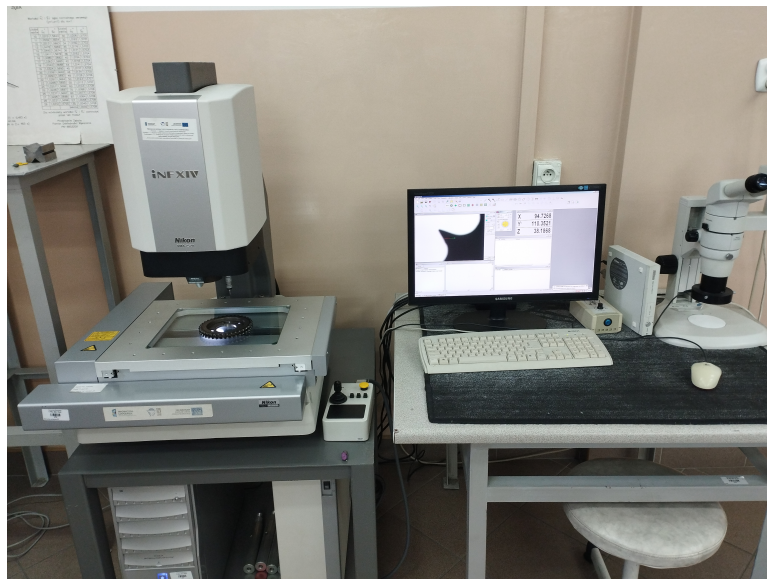


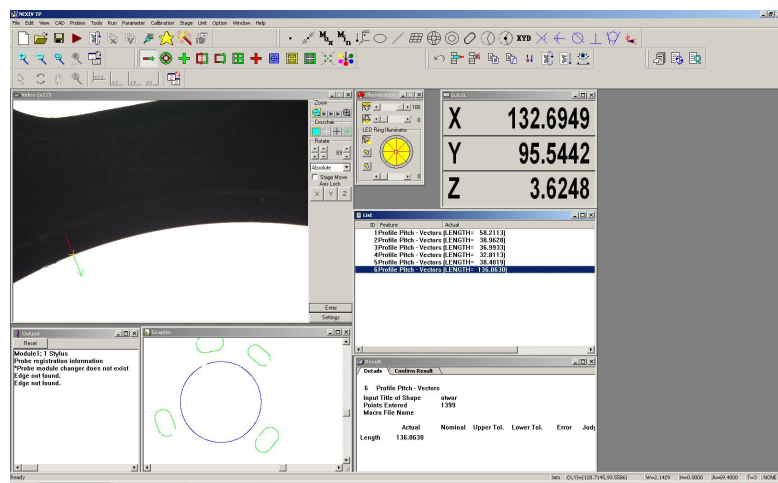
**Figure 1.** Measurement using a contact coordinate measuring system: (a) MarSurf XC 20; (b) measurement of the external profile of the chain wheel; (c) measurement of the internal profile of the chain wheel; (d) measurement of the teeth contour of the chain wheel

Due to the limitations of the MarSurf XC 20 system, the iNEXIV VMA 2520 optical microscope in subgraph (a) of Figure 2 was used to collect the remaining necessary geometrical dimensions of the chain wheel. This device, equipped with a vision system, had its lighting and video preview focus carefully adjusted during the measure. After defining the measurement segment on the video preview, the program was executed automatically. This allowed for the registration of the contours of geometric features inside the chain wheel (internal diameter in subgraph (b) of Figure 2 and slots in subgraph (c) of Figure 2), which was possible due to edge detection based on gray level analysis in the video preview. The highest possible measurement resolution concerning the geometric dimensions of the measured chain wheel was employed, which was 0.01 mm.

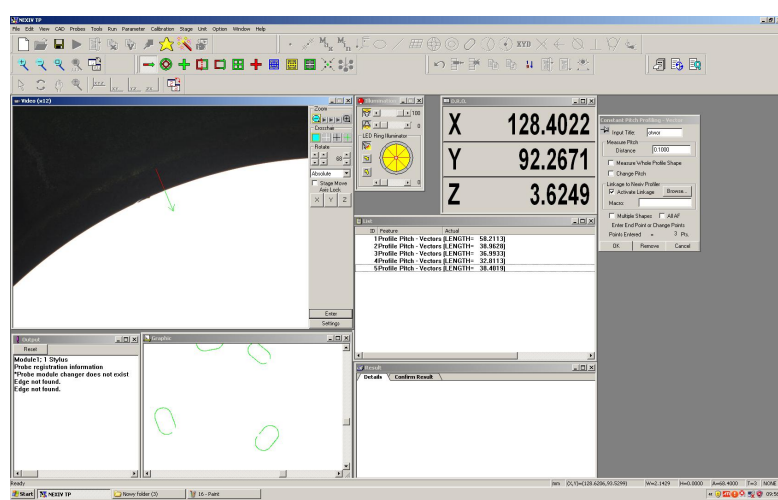
The dimensions of geometric features, inaccessible by the iNEXIVE VMA 2520 microscope and the MarSurf XC 20, were obtained using a digital micrometer in subgraph (a) of Figure 3 and a digital caliper in subgraph (b) of Figure 3.



(a)



(b)



(c)

**Figure 2.** Optical measurement: (a) iNEXIVE VMA 2520 system; (b) measurements of the interior diameter of the chain wheel; (c) measurements of the slots



(a)



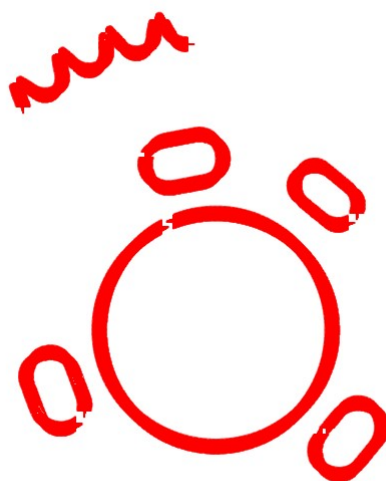
(b)

**Figure 3.** Measurement using manual instruments: (a) digital micrometer; (b) digital caliper

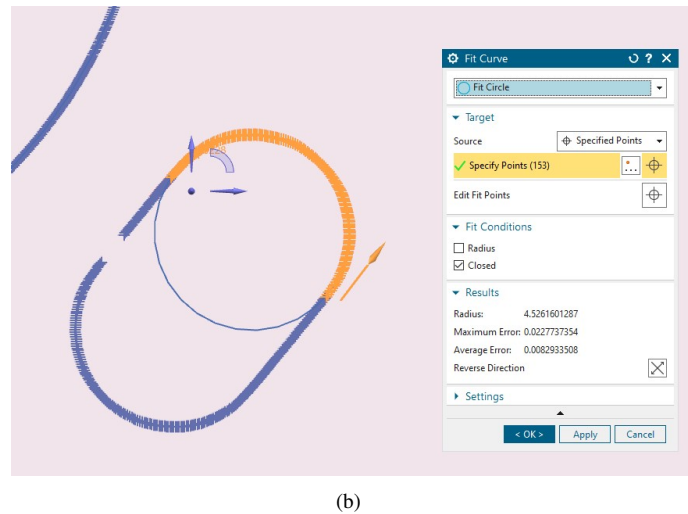
Subsequent geometry reconstruction was performed in the CAD NX software by importing the scanning results. Initially, data obtained from the optical microscope were imported in subgraph (a) of Figure 4. After projecting these points onto the datum plane, suitable curves were generated using the “Fit Curve” function. Slots were made with the “Fit Circle” subfunctions subgraph (b) of Figure 4, and tangents to the resultant circles were drawn in subgraph (c) of Figure 4 upon projecting onto the sketch. Unwanted curves were eliminated using the “Trim” function, and the inner hole was constructed using the “Fit Circle” subfunction.

Data from the MarSurf XC 20 was also incorporated into the NX program. Initially, the contours of several teeth were generated. Teeth fillets and root land were created using the “Fit Circle” subfunction in subgraph (a) of Figure 5, and the teeth profiles with the “Fit Spline” in subgraph (b) of Figure 5. The “Pattern Feature” function was employed to create a circular pattern. The curves defining the upper profile of the circle were constructed using the “Fit Spline” subfunction, and the tooth side relief with the “Fit Spline” in subgraph (c) of Figure 5. In the subsequent step, the created curves were projected onto a sketch to combine them with the contours obtained from the optical microscope. Ultimately, a notch was made between the rows of the chain wheel, utilizing dimensions obtained from measurements with a digital caliper.

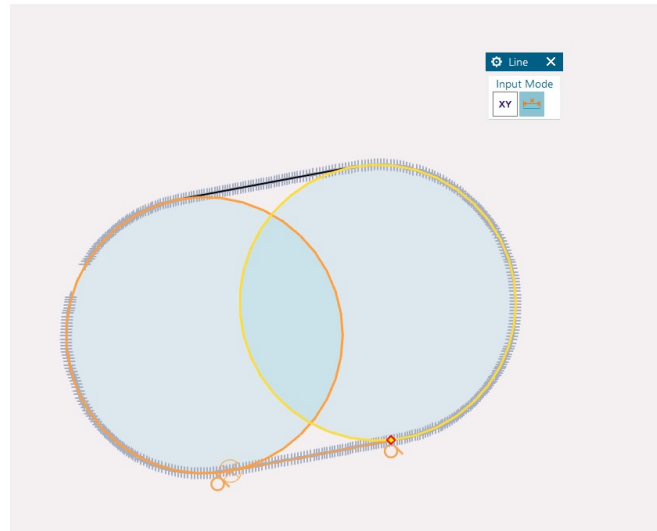
It is noteworthy to mention that when processing more than 1,000 points, the performance of the NX software saw a significant decrease. Consequently, this necessitated the processing of points individually. The points employed in curve creation were allotted to the corresponding layer and subsequently concealed. This approach culminated in a comprehensive reconstruction of the geometry as shown in Figure 6.



(a)

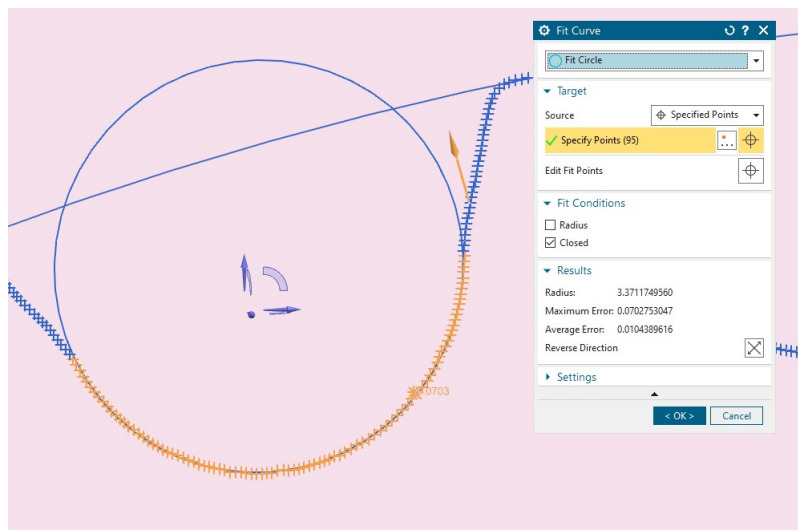


(b)



(c)

**Figure 4.** CAD modeling of data obtained from iNEXIVE system: (a) view of the imported data; (b) Fit Circle option; (c) Tangents to Circles option



(a)

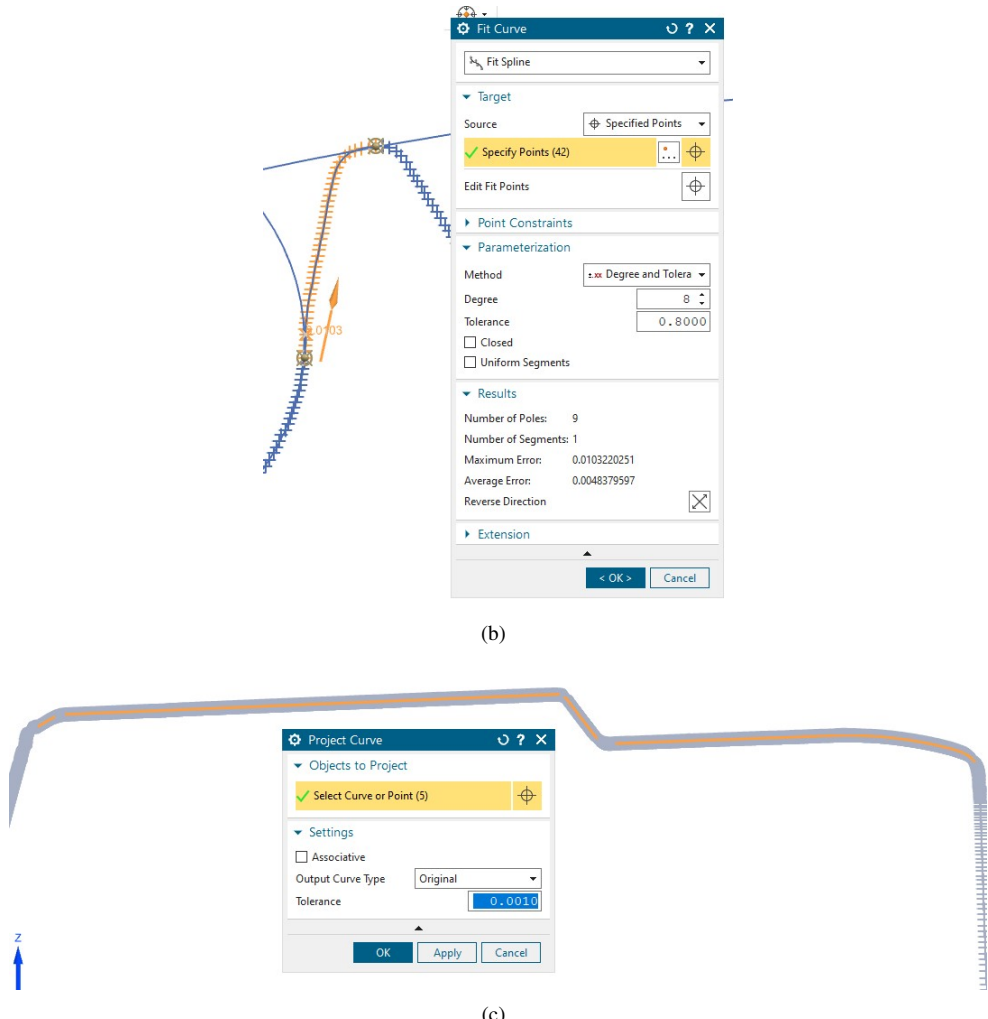


**Figure 5.** Approximation of measured data representing: (a) lower part of teeth; (b) upper part of teeth; (c) upper profile of the chain wheel

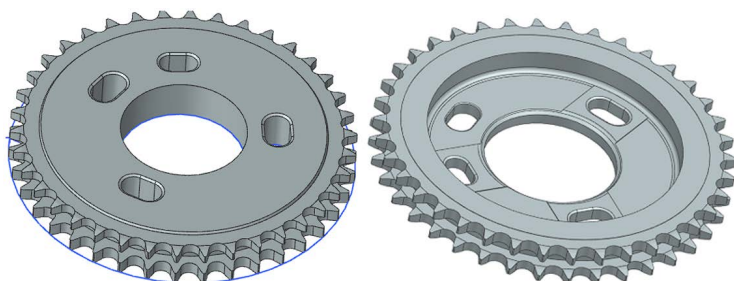


**Figure 6.** View of the reconstructed geometry of the chain wheel

### 3 Results and Discussion

The reconstruction of geometry invariably induces a discrepancy in dimensions compared to the original entity. These discrepancies arise from restrictions embedded within the utilized measurement and computational methodologies, among other factors. The item under examination for geometric measure also harbours inherent manufacturing variations, damage, and wear and tear, often rendering it substantially distinct from its original version. Currently, it remains a daunting task to accurately predict the extent to which the outcome of geometric reconstruction diverges from nominal specifications. Consequently, this study undertakes a comparative analysis of results gleaned from the geometry reconstruction process with design computations, utilizing a chain wheel as a representative example. The chain wheel possesses distinctive parameters, as depicted in Figure 7.

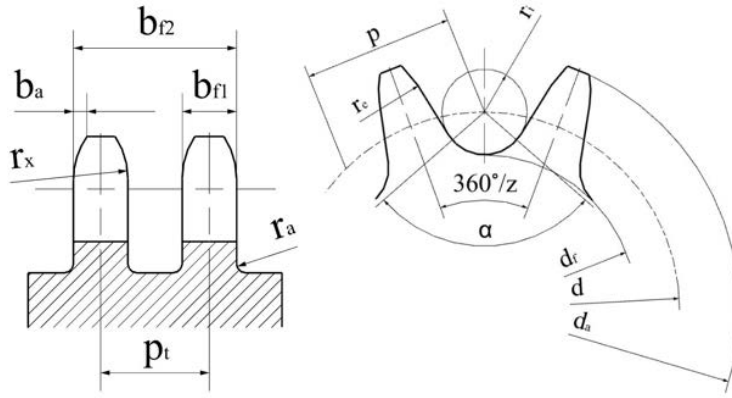


**Figure 7.** The characteristic dimension of the chain wheel

An ISO 606 standard [26] chain, showcasing the nearest pitch value, was employed for computational purposes. Contrarily, certain dimensions, such as transverse pitch or inner link width, were chosen such that they closely aligned with data obtained from measurements. The final results were rounded off to one decimal place, save for the pitch diameter, which was rounded to two decimal places. Table 1 collates the comparison outcomes. Even after meticulous surface cleansing using a cloth and WD 40 grease, the chain wheel still retained residual scratches and dents. Surface cleaning could potentially be augmented through the usage of other cleaning agents or soft-bristle brushes, facilitating the effective removal of impurities without inflicting surface scratches. However, pre-existing wear and tear could not be remedied. As such, measurements recorded not only dimensional and geometrical errors inherent to the chain wheel but also wear-induced defects. Another crucial factor contributing to differences in Table 1 results was the incorporation of varying measurement methodologies, necessitated by the inability of a singular system or tool to digitize all requisite geometrical dimensions defining the gear wheel. This resulted in divergent outcomes, tainted by measurement device errors. Additionally, data derived from measurements using the iNEXIVE microscope and the MarSurf XC 20 measuring station were represented in different coordinate systems, necessitating a conversion to a common system within the NX Siemens program for comprehensive geometry reconstruction. The NX Siemens software's point processing is also error-prone, as all operations are primarily contingent upon the operator's expertise and the CAD software's algorithms. It became imperative during work in the NX program to parameterize the acquired contours, which approximated their characteristic curves. In the case of the circle's most crucial part, i.e., the teeth contour, an initial application of the "Fit Spline" proved unsatisfactory, leading to the introduction of the "Fit Circle" option in this contour part. This procedure facilitated a more accurate profile reconstruction in subgraph (a) of Figure 5. For other contours, the "Fit Line" and "Fit Circle" functions were primarily applied. Though these functions permitted a more accurate reconstruction of the obtained measurement data, their alignment with the set of measurement points demanded a substantial investment of time.

**Table 1.** List of the characteristic dimension

Parameter	Symbol	Calculated data	Measured data
Chain pitch [mm]	$p$	9.525	9.59
Pitch circle diameter [mm]	$d$	115.34	116.13
Top diameter [mm]	$d_a$	119.4 – 122.2	120.2
Root circle diameter [mm]	$d_f$	110.3	109.6
Roller contact angle [ $^{\circ}$ ]	$\alpha$	117.6 – 137.6	132.8
Tooth profile radius [mm]	$r_e$	24.4 – 66	28.9
Tooth radius [mm]	$r_i$	2.6 – 2.7	3.3
Tooth side relief [mm]	$b_a$	1 – 1.4	0.5
Distance between the pitch diameter and the absolute shroud diameter [mm]	$f$	6.7	6.5
Shroud radius [mm]	$r_a$	$\leq 0.8$	0.8
Absolute shroud diameter [mm]	$d_g$	$\leq 102$	103.1
Tooth side radius [mm]	$r_x$	$\geq 9.5$ lub $\geq 7.6$	7.9

## 4 Conclusions

With its advanced contour measurement technology, the MarSurf XC 20 in subgraph (a) of Figure 1 and optical measurement methodologies were utilized in this endeavor. The results obtained from the model generated via the reverse engineering process do not deviate significantly from the model produced during design computations. However, future research endeavors are required to eliminate residual errors and optimize the process for parameters outside the recommended tolerance.

## Data Availability

The data used to support the findings of this study are available from the corresponding author upon request.

## Conflicts of Interest

The authors declare that they have no conflicts of interest.

## References

- [1] M. A. Boboulos, *CAD-CAM & Rapid Prototyping Application Evaluation*. Bookboon, 2010.
- [2] J. D. Camba, M. Contero, and P. Company, “Parametric CAD modeling: An analysis of strategies for design reusability,” *Comput. Aided Des.*, vol. 74, pp. 18–31, 2016. <https://doi.org/10.1016/j.cad.2016.01.003>
- [3] K. Amadori, M. Tarkian, J. Olvander, and P. Krus, “Flexible and robust CAD models for design automation,” *Adv. Eng. Inform.*, vol. 26, no. 2, pp. 180–195, 2012. <https://doi.org/10.1016/j.aei.2012.01.004>
- [4] A. Kumar, P. K. Jain, and P. M. Pathak, “Reverse engineering in product manufacturing: An overview,” *DAAAM Int. Sci. Book*, vol. 39, pp. 665–678, 2013. <https://doi.org/10.2507/daaam.scibook.2013.39>
- [5] E. Bagci, “Reverse engineering applications for recovery of broken or worn parts and re-manufacturing: Three case studies,” *Adv. Eng. Softw.*, vol. 40, no. 6, pp. 407–418, 2009. <https://doi.org/10.1016/j.advengsoft.2008.07.003>
- [6] I. G. E. Fedorova, T. S. Filimonova, E. V. E. Zhuravlev, and V. V. Vasiliev, “Estimation of the possibility of using reverse engineering in the aviation industry,” *Comput. Nanotechnol.*, vol. 6, no. 3, pp. 68–73, 2019. <https://doi.org/10.33693/2313-223x-2019-6-3-68-73>
- [7] M. Dubravcik and S. Kender, “Application of reverse engineering techniques in mechanics system services,” *Proc. Eng.*, vol. 48, pp. 96–104, 2012. <https://doi.org/10.1016/j.proeng.2012.09.491>
- [8] M. Acher, A. Cleve, P. Collet, P. Merle, L. Duchien, and P. Lahire, “Reverse engineering architectural feature models,” in *Software Architecture: 5th European Conference, ECSA 2011, Essen, Germany, September 13–16, 2011*, pp. 220–235. [https://doi.org/10.1007/978-3-642-23798-0\\_25](https://doi.org/10.1007/978-3-642-23798-0_25)
- [9] P. Turek, “Evaluation of the auto surfacing methods to create a surface body of the mandible model,” *Rep. Mech. Eng.*, vol. 3, no. 1, pp. 46–54, 2021. <https://doi.org/10.31181/rme200103046p>
- [10] M. Stojkovic, M. Veselinovic, N. Vitkovic, D. Marinkovic, M. Trajanovic, S. Arsic, and M. Mitkovic, “Reverse modelling of human long bones using T-splines-case of tibia,” *Teh. Vjesn.*, vol. 25, pp. 1753–1760, 2018. <https://doi.org/10.17559/tv-20180129210021>
- [11] P. Turek, “Automating the process of designing and manufacturing polymeric models of anatomical structures of mandible with industry 4.0 convention,” *Polimery*, vol. 64, pp. 522–529, 2019. <https://doi.org/10.14314/polimery.2019.7.9>
- [12] J. Milovanovic, N. Vitkovic, M. Stojkovic, and M. Mitkovic, “Designing of patient-specific implant by using subdivision surface shaped on parametrized cloud of points,” *Teh. Vjesn.*, vol. 28, no. 3, pp. 801–809, 2021. <https://doi.org/10.17559/tv-20200502215442>
- [13] N. Korunovic, D. Marinkovic, M. Trajanovic, M. Zehn, M. Mitkovic, and S. Affatato, “In silico optimization of femoral fixator position and configuration by parametric CAD model,” *Materials*, vol. 12, no. 14, p. 2326, 2019. <https://doi.org/10.3390/ma12142326>
- [14] M. Stojković, M. Trifunović, J. Milovanović, and S. Arsić, “User defined geometric feature for the creation of the femoral neck enveloping surface,” *Facta Univ. Ser. Mech. Eng.*, vol. 20, no. 1, pp. 127–143, 2022. <https://doi.org/10.22190/FUME200220034S>
- [15] L. Ciocca, S. Mazzoni, M. Fantini, F. Persiani, P. Baldissara, C. Marchetti, and R. Scotti, “A CAD/CAM-prototyped anatomical condylar prosthesis connected to a custom-made bone plate to support a fibula free flap,” *Med. Biol. Eng. Comput.*, vol. 50, pp. 743–749, 2012. <https://doi.org/10.1007/s11517-012-0898-4>
- [16] Y. F. Liu, L. W. Xu, H. Y. Zhu, and S. S. Liu, “Technical procedures for template-guided surgery for mandibular reconstruction based on digital design and manufacturing,” *Biomed. Eng. Online*, vol. 13, pp. 1–15, 2014. <https://doi.org/10.1186/1475-925x-13-63>

- [17] J. S. E. Milovanović, M. Stojković, M. Trifunović, and N. Vitković, “Review of bone scaffold design concepts and design methods,” *Facta Univ. Ser. Mech. Eng.*, 2020. <https://doi.org/10.22190/FUME200328038M>
- [18] G. D. Barai, S. S. Shete, and L. P. Raut, “Design and development of a component by reverse engineering,” *IJRET*, vol. 4, no. 5, pp. 539–546, 2015. <https://doi.org/10.15623/ijret.2015.0405100>
- [19] S. H. Mian, M. A. Mannan, and A. Al-Ahmari, “Accuracy of a reverse-engineered mould using contact and non-contact measurement techniques,” *Int. J. Comput. Integr. Manuf.*, vol. 28, no. 5, pp. 419–436, 2015. <https://doi.org/10.1080/0951192x.2014.880800>
- [20] R. H. Helle and H. G. Lemu, “A case study on use of 3D scanning for reverse engineering and quality control,” *Mater. Today: Proc.*, vol. 45, pp. 5255–5262, 2021. <https://doi.org/10.1016/j.matpr.2021.01.828>
- [21] T. Brajlih, T. Tasic, I. D. Igor, B. Valentan, M. Hadzistevic, V. Pogacar, J. Balic, and B. Acko, “Possibilities of using three-dimensional optical scanning in complex geometrical inspection,” *J. Mech. Eng.*, vol. 57, no. 11, pp. 826–833, 2011. <https://doi.org/10.5545/sv-jme.2010.152>
- [22] P. Zhao, X. W. Bai, Y. K. Li, Y. Li, and C. Y. Lv, “A new method of data smoothing for scan-line point cloud in reverse engineering,” *Adv. Mater. Res.*, vol. 1006, pp. 352–355, 2014. <https://doi.org/10.4028/www.scientific.net/amr.1006-1007.352>
- [23] R. Gu, A. Sun, Y. Li, and Z. Wang, “An analysis of triangulation reconstruction based on 3D point cloud with geometric features,” in *Tenth Int. Symp. Precis. Mech. Meas., Qingdao, China*, 2021, pp. 582–588. <https://doi.org/10.1117/12.2616832>
- [24] P. Turek and G. Budzik, “Development of a procedure for increasing the accuracy of the reconstruction and triangulation process of the cranial vault geometry for additive manufacturing,” *Facta Univ., Ser. Mech. Eng.*, 2022. <http://dx.doi.org/10.22190/FUME211208025T>
- [25] D. Brujic, I. Ainsworth, and M. Ristic, “Fast and accurate nurbs fitting for reverse engineering,” *Int. J. Adv. Manuf. Technol.*, vol. 54, pp. 691–700, 2011. <https://doi.org/10.1007/s00170-010-2947-1>
- [26] ISO, “Short pitch transmission precision roller chains and chain wheels,” International Standard ISO 606, 2015.